

Purification and unique properties of mammary epithelial stem cells

John Stingl^{1,3}, Peter Eirew¹, Ian Ricketson¹, Mark Shackleton⁴, François Vaillant⁴, David Choi¹, Haiyan I. Li² & Connie J. Eaves^{1,5}

Elucidation of the cellular and molecular mechanisms that maintain mammary epithelial tissue integrity is of broad interest and paramount to the design of more effective treatments for breast cancer¹. Evidence from both *in vitro* and *in vivo* experiments suggests that mammary cell differentiation is a hierarchical process originating in an uncommitted stem cell with self-renewal potential^{2–4}. However, analysis of the properties and regulation of mammary stem cells has been limited by a lack of methods for their prospective isolation. Here we report the use of multi-parameter cell sorting and limiting dilution transplant analysis to demonstrate the purification of a rare subset of adult mouse mammary cells that are able individually to regenerate an entire mammary gland within 6 weeks *in vivo* while simultaneously executing up to ten symmetrical self-renewal divisions. These mammary stem cells are phenotypically distinct from and give rise to mammary epithelial progenitor cells that produce adherent colonies *in vitro*. The mammary stem cells are also a rapidly cycling population in the normal adult and have molecular features indicative of a basal position in the mammary epithelium.

The mammary gland develops after birth from a small number of invading cells derived from the ectoderm⁵. These cells then generate a series of branching ducts that terminate in sac-like lobules embedded in stromal tissue. The structures produced are composed of a continuous epithelium consisting of an outer basal layer of contractile myoepithelial cells and an inner layer of luminal cells. Experiments with retrovirally marked mouse mammary cells transplanted into cleared mammary fat pads have established the existence of mammary stem cells that are able to regenerate new mammary tissue *in vivo* and display self-renewal activity². Here we refer to such cells operationally as mammary repopulating units (MRUs). Mammary glands also contain different types of progenitor cells that can be detected under various conditions *in vitro*^{3,6,7}. Mammary colony-forming cells (Ma-CFCs) refer to those progenitors that produce discrete colonies of mammary cells in low-cell density adherent cultures⁷. At present, little is known about the biological properties of MRUs, or the mechanisms that regulate their behaviour and relationship to mammary cells that proliferate *in vitro*. Investigation of these key questions is essential to developing an understanding of mammary stem cell fate decisions and transformation. To begin to address these, we analysed the phenotypic and cycling properties of cells detectable *in vivo* as MRUs and compared them to cells detectable *in vitro* as Ma-CFCs.

In preliminary experiments we found that MRUs could be routinely detected in single cell suspensions prepared by enzymatic digestion of adult mouse mammary tissue and regenerated macroscopic mammary outgrowths within 6 weeks after injection into cleared mammary fat pads of weaning female mice⁸. The outgrowths produced (Fig. 1a, b)

were histologically normal (Fig. 1c) and contained both mature keratin 18-expressing luminal cells and smooth muscle actin-positive myoepithelial cells (Fig. 1d). *In vitro* assays of single cell suspensions prepared from such regenerated outgrowths demonstrated that they also contained numerous Ma-CFCs (Fig. 1e), thus demonstrating a parent–progeny relationship between MRUs and Ma-CFCs.

To investigate whether reaggregation of dissociated cells is an essential step in the formation of MRU-derived outgrowths, small numbers of cells from green fluorescent protein (GFP)⁹ and cyan fluorescent protein (CFP)¹⁰ donors were mixed together and transplanted. Most outgrowths produced from these mixed transplants were found to contain either GFP⁺ or CFP⁺ Ma-CFCs, but not both genotypes (Fig. 1e), providing strong support for the view that single cells can generate complete outgrowths. Formal proof of this concept was obtained from the results of single cell transplants using highly purified MRUs (Fig. 1f and Supplementary Fig. 1; see below for the phenotype selection strategy and MRU purity achieved). In these experiments, the purified cells were first placed at a low concentration in a multiwell plate and the contents of wells containing only one cell then selected by microscopic inspection before being individually harvested and injected into cleared fat pads. The ability of a single cell to generate an outgrowth (Fig. 1f) indicates that MRUs can display their regenerative potential in the absence of any co-injected cells.

Consistent with these findings, we observed a negative linear relationship between the transplant cell dose and the log proportion of cleared fat pads that did not contain outgrowths when the number of cells injected was varied (Fig. 1g). This relationship also validated the use of limiting dilution analysis to quantify MRUs in variously manipulated suspensions of mammary cells. The frequency of MRUs in single cell suspensions obtained from adult virgin female FVB mouse inguinal mammary glands dissociated using an 8-h enzymatic procedure was determined by limiting dilution analysis to be 1 MRU per 1,400 dissociated cells (95% confidence interval = 1 per 600 to 1 per 3,000 cells, Supplementary Table 1). The total yield of viable cells obtained by this dissociation procedure was approximately 2 million per gland. Therefore, each inguinal gland contains at least 1,400 MRUs and probably more considering the imperfect yield of single cells expected from the dissociation procedure used. Similar values were determined for the frequency and yield of MRUs in cell suspensions obtained from the mammary glands of C57Bl/6 mice (Fig. 1e), indicating the reproducibility of these values between strains. Notably, when the same inguinal mammary gland cell suspensions were assayed *in vitro*, Ma-CFCs were detected at a 20-fold higher frequency (that is, 1 Ma-CFC per 63 cells (\pm s.e.m. = 1 per 45 to 1 per 108), indicating a yield of approximately 30,000 Ma-CFCs per gland) in comparison to the values obtained for

¹Terry Fox Laboratory, and ²Michael Smith Genome Sciences Centre, British Columbia Cancer Agency, Vancouver V5Z 1L3, British Columbia, Canada. ³StemCell Technologies Inc., Vancouver V5Z 1B3, British Columbia, Canada. ⁴The Walter and Eliza Hall Institute of Medical Research, WEHI Biotechnology Centre, Parkville, Victoria 3050, Australia. ⁵Departments of Medical Genetics, Pathology and Laboratory Medicine, and Medicine, University of British Columbia, Vancouver V6T 1Z3, British Columbia, Canada.

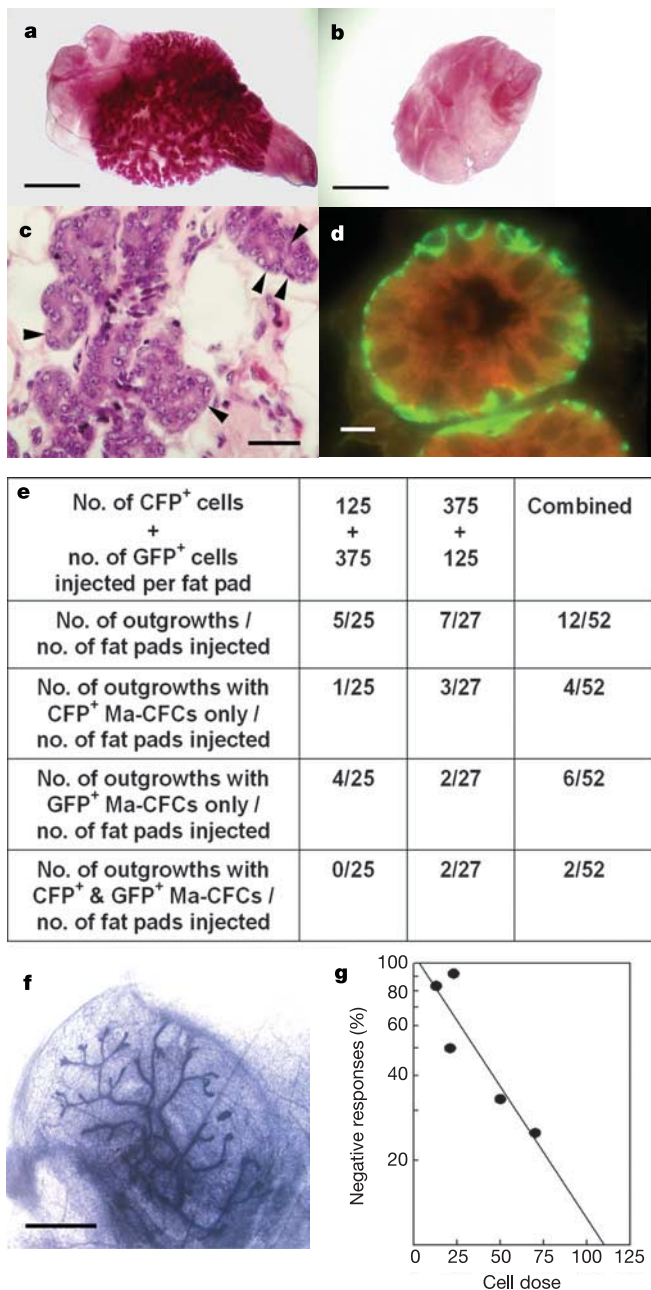


Figure 1 | The MRU assay. **a**, Mammary gland outgrowth produced in a transplanted fat pad. Scale bar, 0.25 cm. **b**, Cleared fat pad not injected with cells. Scale bar, 0.25 cm. **c**, Stratified epithelium visualized in a haematoxylin and eosin-stained gland obtained in a fat pad injected with 12 CD45⁺ Ter119⁻ CD31⁻ Sca-1^{low} CD24^{med} CD49f^{high} cells. Arrowheads indicate myoepithelial cells. Scale bar, 25 μ m. **d**, Regenerated gland showing keratin 18-positive luminal cells (red) and smooth muscle actin-positive myoepithelial cells (green). Scale bar, 10 μ m. **e**, Proportions of outgrowths produced in fat pads transplanted with a mixture of GFP⁺ and/or CFP⁺ cells (see Supplementary Methods) that contained GFP⁺ and/or CFP⁺ Ma-CFCs. Frequencies of MRUs in the original GFP⁺ and CFP⁺ suspensions were 1 per 1,500 (95% confidence interval = 1 per 700 to 1 per 3,000) and 1 per 2,000 (95% confidence interval = 1 per 910 to 1 per 4,500). The probability of obtaining a mixed outgrowth given these individual frequencies was 0.015 (not significantly different from the observed outcome of 2 per 52 = 0.04, $P = 0.19$). **f**, A mammary gland regenerated in a fat pad of a virgin host injected with a single CD45⁺ Ter119⁻ CD31⁻ Sca-1^{low} CD24^{med} CD49f^{high} cell (one positive fat pad of 77 injected with single cells). Scale bar, 1 mm. **g**, Negative linear relationship between the number of CD45⁺ Ter119⁻ CD31⁻ CD140a⁻ CD24^{med} CD49f^{high} mammary cells transplanted and the proportion of negative fat pads obtained. The goodness of fit of this model was confirmed ($P = 0.40$).

MRUs. These findings suggested that MRUs represent a much rarer cell type than Ma-CFCs.

To characterize MRUs further, we analysed their distribution in various subpopulations of cells from enzymatically digested mammary glands that could be isolated using the fluorescence activated cell sorter (FACS) after staining the cells with antibodies to various surface markers. Markers examined included Sca-1, a marker previously described to identify MRUs¹¹; CD24, a marker for which the absence characterizes human mammary tumour stem cells¹; and CD49f, a marker expressed by epidermal stem cells^{12,13} and human Ma-CFCs⁷. In human mammary tissue, CD24 has been localized to the apical plasma membrane of the luminal cells¹⁴, although similar studies of mouse mammary tissue suggested a more ubiquitous pattern of expression (Fig. 2a). In contrast, CD49f is most highly expressed by cells of the basal layer of skin epithelial cells¹⁵, and a basal pattern of expression was confirmed here for the mouse mammary gland (Fig. 2b). We found that when contaminating haematopoietic (CD45⁺ and Ter119⁺) cells were first removed and then the most highly CD49f⁺ (CD49f^{high}) cells were selected (Fig. 2c), either with or without simultaneous selection of the Sca-1^{low} subset (cells within the lower-right gate indicated in Fig. 2d), more than 50% of the MRUs in suspensions of FVB mouse mammary cells could be recovered at a sevenfold higher frequency (~1 per 200 cells; 4 positive fat pads out of 6 injected with 200 cells each) than the frequency of MRUs in the initial cell suspension. No MRUs were detected in the Sca-1^{high} subset of CD49f⁺ cells (0 positive fat pads out of 8 injected with 600 cells each from the upper-left gate in Fig. 2d). We did not culture the cells before staining because this induced the expression of Sca-1 on all mammary epithelial cells (Supplementary Fig. 2). Additional removal of contaminating endothelial (CD31⁺) cells and selection of the CD24⁺ subset of the CD45⁻ Ter119⁻ CD31⁻ Sca-1^{low} CD49f^{high} cells (upper population in Fig. 2e) increased the frequency of the MRUs another tenfold (to ~1 per 20 cells; 3 positive fat pads out of 4 injected with 18 of these cells each, and 4 positive fat pads out of 10 injected with 12 of these cells, and 0 positive fat pads out of 12 injected, each with 312 of the corresponding CD24^{low/-} subset, Fig. 2e). Expression of CD24 in MRUs has also been demonstrated previously¹⁶. When stromal (CD140a⁺) cells were also removed but the Sca-1 staining was omitted, approximately 80% of the MRUs were found in a subset of cells that express medium levels of CD24 and high levels of CD49f (CD45⁻ Ter119⁻ CD31⁻ CD140a⁻ CD24^{med} CD49f^{high} cells). In this subset, the frequency of MRUs was 1 per 60 cells (from FVB mice) and 1 per 90 cells (from C57Bl/6 mice) (Fig. 3a and Supplementary Table 2). Accordingly, this fraction has been labelled in Fig. 3a as 'MRU'. The few remaining MRUs were found to have a CD24^{low} CD49f^{low} phenotype. Because immunostaining (Fig. 2b) demonstrated that differentiated myoepithelial cells express both CD24 and CD49f, the CD24^{low} CD49f^{low} fraction shown in Fig. 3a was labelled as 'MYO' (anticipating that it would be enriched in its content of myoepithelial cells).

Ma-CFCs, like MRUs, were found to co-express both CD24 and CD49f (Fig. 4a). However, they differ from MRUs in that most Ma-CFCs (90%) were found in the CD24^{high} CD49f^{low} population that lacks detectable MRUs. Hence we labelled the CD24^{high} CD49f^{low} fraction shown in Fig. 3a as 'Ma-CFC'. We also examined the types of colonies produced by cells from the Ma-CFC-enriched and MRU-enriched fractions after 16 days of growth in Matrigel cultures. The colonies generated by cells from the Ma-CFC-enriched fraction had a uniformly spherical acinar structure composed of a simple cuboidal epithelium (top panels in Fig. 3b). In contrast, cells from the MRU-enriched fraction produced solid, irregular-shaped colonies and occasional large colonies with a branched ductal appearance and an irregular-shaped lumen (Fig. 3b, lower panels).

The ability to prospectively isolate distinct, highly enriched populations of MRUs and Ma-CFCs afforded an opportunity to look for differences in their gene expression profiles and to compare

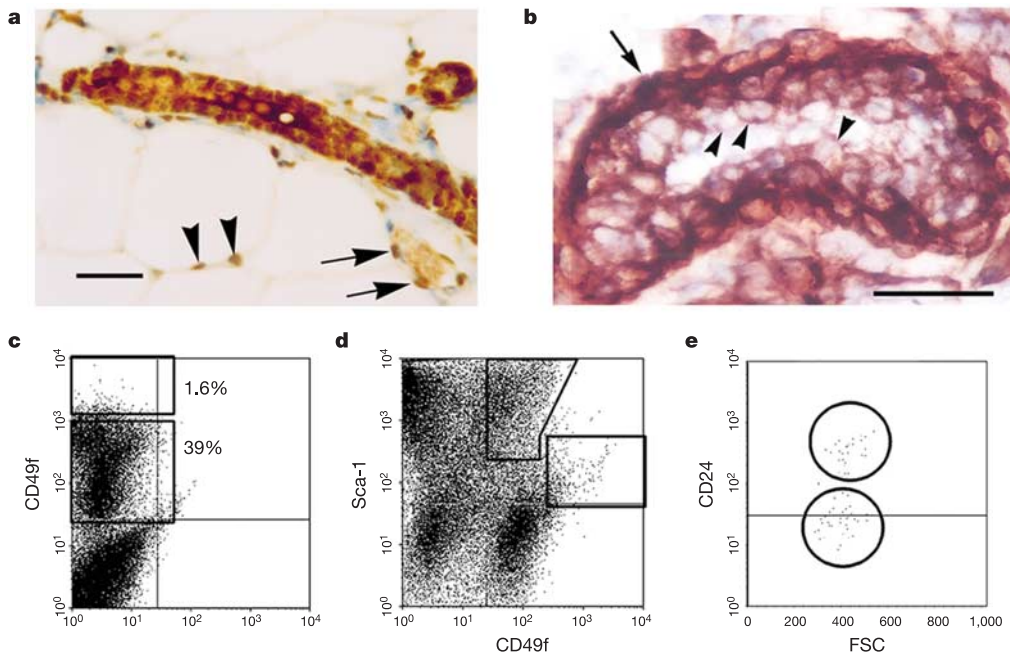


Figure 2 | Phenotypic characterization of MRUs.
a, CD24⁺ epithelial cells, adipocytes (arrowheads) and endothelial cells (arrows). Scale bar, 25 μ m. **b**, CD49f expression is higher in basal cells (arrow) than in luminal cells (arrowheads). Scale bar, 25 μ m. **c–e**, FACS dot plots showing the distribution of mammary cells according to their expression of various markers. **c**, CD49f and gates used to distinguish CD49f^{low} and CD49f^{high} cells. **d**, CD49f and Sca-1. **e**, CD24 (and forward light scattering (FSC) characteristics) within the CD45⁺Ter119⁻CD31⁻Sca-1^{low}CD49f^{high} population.

these to the MYO population that contains very few cells able to produce outgrowths in cleared fat pads or adherent colonies *in vitro*. Hybridization of amplified RNA from each of these subsets to Affymetrix mouse MOE430 genome array chips indicated that the Ma-CFC-enriched cells contain higher levels of keratin 8, 18 and 19 transcripts and a variety of casein transcripts also typical of luminal cells, in comparison to either the MRU-enriched or MYO cells (Supplementary Tables 5–7). Conversely, transcripts for keratins 5 and 14, smooth muscle actin, smooth muscle myosin, vimentin and laminin, all of which show elevated expression in basal/myoepithelial cells, were found to be present at higher levels in the MRU-enriched and MYO populations. However, significant differences in gene expression were not evident when the latter two fractions were compared. The differences in keratin 14, 18 and 19 and smooth muscle actin transcript levels in the three populations studied

were confirmed by quantitative real-time PCR analysis (Fig. 3c). Notably, transcripts for keratin 6, a putative progenitor cell marker¹⁷, were also found to be highest in the fraction enriched in Ma-CFCs (Fig. 3c).

Immunostaining of individual cells in the highly MRU-enriched fraction indicated that some expressed two markers associated with basal cells (23% positive for smooth muscle actin, $n = 620$; 27% for keratin 14, $n = 600$). Others expressed markers associated with luminal cells (18% positive for keratin 18), but none (<0.1%) co-expressed markers of both lineages and approximately half did not express any of these (Fig. 3d). Immunostaining of cells isolated from the same three fractions with an antibody to keratin 6 confirmed the PCR results with 49% positive cells in the Ma-CFC-enriched fraction as compared to 0–2% positive cells in the MRU-enriched and MYO fractions (Fig. 3e).

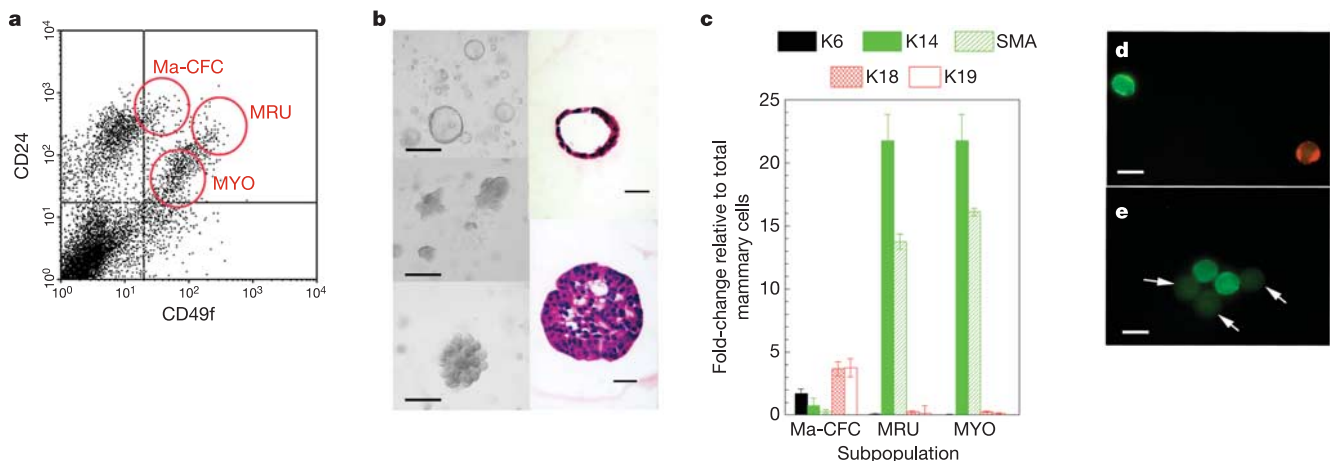


Figure 3 | Functional and molecular characterization of subsets of mammary cells. **a**, Distribution of CD45⁺Ter119⁻CD31⁻CD140a⁻ cells according to their CD24 and CD49f expression. **b**, Gross morphology (left) and haematoxylin and eosin-stained sections (right) of colonies produced in Matrigel cultures from CD24^{high}CD49f^{low} cells (Ma-CFC fraction, top panel) and from CD24^{med}CD49f^{high} cells (MRU fraction, middle and bottom panels). Scale bars, 2 mm (left panels) and 20 μ m (right panels).

c, Quantitative real-time PCR analysis of transcript levels in different subpopulations (mean \pm s.e.m. of data from three independent isolates as compared to unfractionated mammary gland cells). K, keratin. **d**, Immunostaining of FACS-purified CD45⁺Ter119⁻CD31⁻CD49f^{high} cells (MRU fraction) for expression of keratin 14 (green) and keratin 18 (red). Scale bar, 10 μ m. **e**, Keratin 6⁺ CD24^{high}CD49f^{low} cells (Ma-CFC fraction). Arrows indicate autofluorescence; scale bar, 10 μ m.

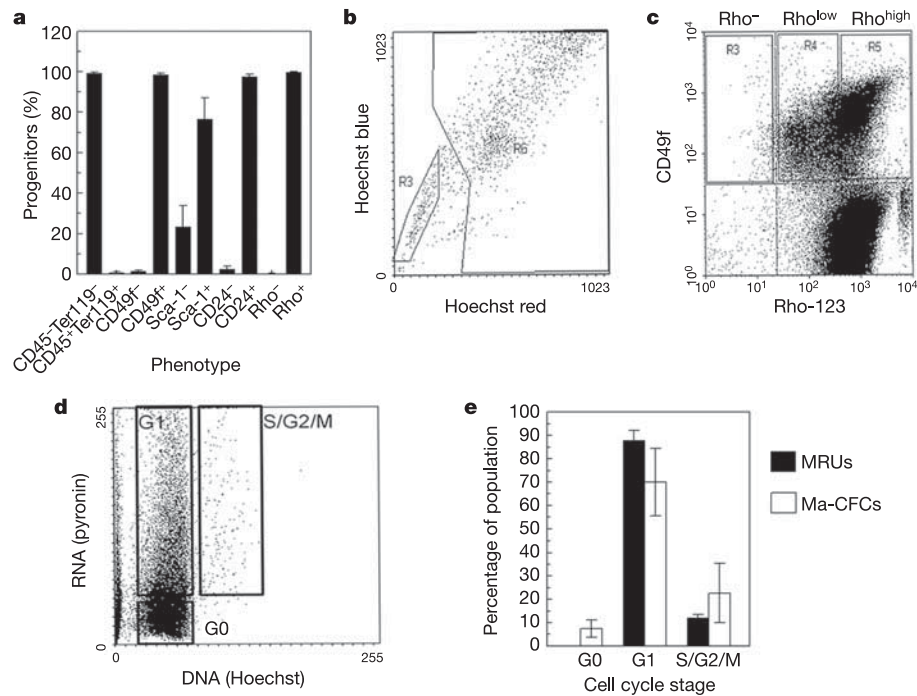


Figure 4 | Characterization of dye efflux and cycling properties of MRUs and Ma-CFCs. **a**, Percentage (\pm s.e.m.) of Ma-CFCs in subpopulations indicated. **b**, Distribution of CD45⁺Ter119⁻CD49f⁺ mammary cells according to their Hoechst 33342 fluorescence (left gate, side population; right gate, non-side population). **c**, Distribution of mammary cells according to their CD49f expression and Rho efflux activity. **d**, Distribution

of CD45⁺ mammary cells in G0, G1 and S/G2/M determined by Hoechst 33342/pyronin Y staining. These fractions contained $38 \pm 11\%$, $59 \pm 11\%$ and $3 \pm 1\%$ (mean \pm s.e.m.), respectively, of all the CD45⁺ cells. **e**, Percentage (\pm s.e.m.) of MRUs and Ma-CFCs in the G0, G1 and S/G2/M fractions.

To further characterize MRUs and Ma-CFCs, we examined their Hoechst 33342 and rhodamine-123 (Rho) efflux properties, as well as their distribution in different phases of the cell cycle. Hoechst 33342 is a substrate of Abcg2 and this allows Abcg2⁺ cells to display a unique 'side population' phenotype^{18,19}. Hoechst 33342 and Rho efflux properties are both discriminating features of quiescent murine haematopoietic stem cells²⁰ but these properties are lost when these cells are activated into cycle²¹. Primitive retinal²² and cardiac cells²³, embryonic stem cells¹⁹ and some mammary cells²⁴ have also been reported to possess a side population phenotype. We found that mammary gland preparations also contain a small fraction of side population cells ($1.9 \pm 0.5\%$ (mean \pm s.e.m.) of the total, $n = 7$, Fig. 4b), but these accounted for less than 10% of all the MRUs (Supplementary Table 3). Similarly, a minority of CD49f⁺ mammary cells effluxed Rho (Fig. 4c), and this was also true for both MRUs (Supplementary Table 4) and Ma-CFCs (Fig. 4a). Analysis of Hoechst 33342/pyronin Y-stained mammary cells (Fig. 4d) showed that all of the MRUs and >95% of the Ma-CFCs were present in the G1 or S/G2/M fractions (Fig. 4e). MRUs were also broadly distributed in their forward light scattering characteristics, as expected for a cycling population (data not shown). These findings are consistent with a recent report of a cycling population of mammary epithelial cells thought to be primitive because of their ability to retain ³H-thymidine 5 weeks after a pulse exposure *in vivo*²⁵.

Self-renewal is the hallmark property of stem cells. To examine the self-renewal properties of single MRUs, 34 fat pads were transplanted with low numbers (11–42) of MRU-enriched (CD24^{med}CD49f^{high}) cells. Because outgrowths were produced in only 11 of the 34 fat pads injected, most of these could be assumed to have arisen from a single MRU. Secondary limiting dilution MRU assays were performed on cell suspensions prepared from 4 of these 11 primary outgrowths, and the results demonstrated that they contained 25, 110, 190 and 1,200 MRUs, respectively. Thus, highly purified single

MRUs could be shown to execute at least ten symmetrical self-renewal divisions.

These findings indicate a hierarchy of differentiating cells in the adult mammary gland that includes developmentally distinct and prospectively separable stem and progenitor cell types identified by quantitative *in vivo* and *in vitro* assays. The ability to isolate these cells as distinct populations sets the stage for future delineation of how mammary stem cell self-renewal and differentiation is normally regulated and perturbed during oncogenesis. The high proliferative activity of steady-state MRUs suggests an important role of apoptotic mechanisms in the normal regulation of these cells and may enhance their vulnerability to mutagenic events.

METHODS

Cell preparation. Mammary glands from 8–14-week-old virgin female FVB, C57Bl/6, or congenic GFP⁹ and CFP¹⁰ mice were digested for 8 h at 37 °C in EpiCult-B with 5% fetal bovine serum (FBS), 300 U ml⁻¹ collagenase and 100 U ml⁻¹ hyaluronidase. Prolongation of the period of enzymatic digestion to 16 h resulted in a selective and eightfold overall decrease in MRU yield. After vortexing and lysis of the red blood cells in NH₄Cl, a single cell suspension was obtained by sequential dissociation of the fragments by gentle pipetting for 1–2 min in 0.25% trypsin, and then 2 min in 5 mg ml⁻¹ dispase II plus 0.1 mg ml⁻¹ DNase I (DNase; Sigma) followed by filtration through a 40- μ m mesh. All reagents were from StemCell Technologies Inc. unless otherwise specified.

Cell separation. CD45⁺Ter119⁺, CD31⁺ and CD140a⁺ cells were removed using the EasySep biotin selection kit (StemCell Technologies) after treatment of dissociated cells with 2 μ g ml⁻¹ Fc receptor antibody (2.4G2, American Type Culture Collection) followed by 10 min with a 1:500 dilution of biotinylated StemSep murine/human chimera cocktail (StemCell Technologies), 1 μ g ml⁻¹ biotinylated anti-CD31 (clone MEC13.3, Pharmingen) and 1 μ g ml⁻¹ biotinylated anti-CD140a (clone APA5, eBioscience). In some experiments, cells were incubated for 10 min in 10% rat serum and 10 μ g ml⁻¹ 2.4G2 and then anti-CD45-allophycocyanin (APC, clone 30F11, Pharmingen), anti-CD24-R-phycoerythrin (PE, clone M1/69, Pharmingen), biotinylated anti-CD31, anti-CD49f-PE or fluorescein isothiocyanate (FITC, clone GoH3, Pharmingen), or

APC (R&D Systems) and biotinylated Sca-1 or Sca-1-PE (clone E13-161.7, Pharmingen). Apoptotic cells were excluded by elimination of annexin-V⁺ cells after staining with annexin-V-APC (Pharmingen). For assays of MRUs in sorted populations, viable cell numbers were determined by microscope counts before injecting the cells into cleared fat pads. For transplants of single CD45⁻Ter119⁻CD31⁻Sca-1^{low}CD24^{med}CD49f^{high} cells, these were first distributed at 1 cell per 3 wells in Terasaki plates (Greiner Bio-One) and visually checked before selection for injection. Cells were stained with Rho, or Hoechst 33342 and/or pyronin Y and gates set as previously described^{21,26} with the modification that EpiCult-B with 5% FBS was used during the 37°C incubation step. All sorts were performed using a FACS Vantage or FACS Aria (Becton Dickinson) and gates were set to exclude >99.9% of cells labelled with isoform-matched control antibodies conjugated with the corresponding fluorochromes.

In vitro colony assays. Most Ma-CFCs assays were performed in standard 5–6-day liquid cultures as previously described for human Ma-CFCs²⁷. To assay outgrowths for Ma-CFCs, half of the suspension obtained from each outgrowth was plated in a single dish and the colonies produced 5 days later counted using a regular microscope and genotyped using a fluorescent microscope. All colonies were exclusively GFP⁺ or CFP⁺. In selected experiments, colonies were generated in 50- μ l cultures of Matrigel (Becton Dickinson) covered with 4 ml of Epicult-B medium containing 5% FCS. After 16 days, each 50- μ l Matrigel culture was fixed in 4% paraformaldehyde and then removed intact, embedded in 1% agarose, fixed again in 4% paraformaldehyde, sectioned and stained with haematoxylin and eosin.

In vivo assays in cleared mammary fat pads. Mammary glands of 21-day-old female FVB or C57Bl/6J mice were cleared of endogenous epithelium as previously described²⁸, and test cells in 5–10 μ l of Hanks' balanced salt solution plus 2% FBS with 10% trypan blue (Sigma) were injected into each cleared fat pad. Three weeks after surgery, the mice were mated except in the single cell transplants and some of the mixed donor cell transplants. After a total of 6 weeks, the glands were excised and stained with carmine alum (StemCell Technologies) or haematoxylin for whole-mount analysis. In mice that were mated, only complete outgrowths containing both lobular and ductal elements were scored as a positive, although very few outgrowths containing only one of these elements were seen in several hundred transplants performed. The frequency of MRUs in the cell suspension being transplanted was calculated using Poisson statistics and the method of maximum likelihood using L-Calc software (StemCell Technologies)²⁹. When all fat pads were either positive or negative, an estimate of the MRU frequency range was obtained using one-sided 95% Clopper Pearson limits. Goodness of fit to a single-hit Poisson model was tested with standard Chi-squared statistics.

See Supplementary Methods for details on immunocytochemistry, microarray and quantitative real-time PCR analyses.

Received 12 October; accepted 22 November 2005.

Published online 4 January 2006.

- Al Hajj, M. & Clarke, M. F. Self-renewal and solid tumour stem cells. *Oncogene* **23**, 7274–7282 (2004).
- Kordon, E. C. & Smith, G. H. An entire functional mammary gland may comprise the progeny from a single cell. *Development* **125**, 1921–1930 (1998).
- Dontu, G. *et al.* *In vitro* propagation and transcriptional profiling of human mammary stem/progenitor cells. *Genes Dev.* **17**, 1253–1270 (2003).
- Stingl, J., Raouf, A., Emerman, J. T. & Eaves, C. J. Epithelial progenitors in the normal human mammary gland. *J. Mamm. Gland Biol. Neoplasia* **10**, 49–59 (2005).
- Sakakura, T. in *The Mammary Gland: Development, Regulation, and Function* (eds Neville, M. C. & Daniel, C. W.) 37–66 (Plenum, New York, 1987).
- Smalley, M. J., Tittley, J. & O'Hare, M. J. Clonal characterization of mouse mammary luminal epithelial and myoepithelial cells separated by fluorescence-activated cell sorting. *In Vitro Cell. Dev. Biol. Anim.* **34**, 711–721 (1998).
- Stingl, J., Eaves, C. J., Zandieh, I. & Emerman, J. T. Characterization of bipotent mammary epithelial progenitor cells in normal adult human breast tissue. *Breast Cancer Res. Treat.* **67**, 93–109 (2001).
- Smith, G. H. Experimental mammary epithelial morphogenesis in an *in vivo* model: evidence for distinct cellular progenitors of the ductal and lobular phenotype. *Breast Cancer Res. Treat.* **39**, 21–31 (1996).
- Wagers, A. J., Sherwood, R. I., Christensen, J. L. & Weissman, I. L. Little evidence for developmental plasticity of adult hematopoietic stem cells. *Science* **297**, 2256–2259 (2002).
- Hadjantonakis, A. K., Macmaster, S. & Nagy, A. Embryonic stem cells and mice expressing different GFP variants for multiple non-invasive reporter usage within a single animal. *BMC Biotechnol.* **2**, 11 (2002).
- Wlem, B. E. *et al.* Sca-1^{pos} cells in the mouse mammary gland represent an enriched progenitor cell population. *Dev. Biol.* **245**, 42–56 (2002).
- Tani, H., Morris, R. J. & Kaur, P. Enrichment for murine keratinocyte stem cells based on cell surface phenotype. *Proc. Natl Acad. Sci. USA* **97**, 10960–10965 (2000).
- Li, A., Simmons, P. J. & Kaur, P. Identification and isolation of candidate human keratinocyte stem cells based on cell surface phenotype. *Proc. Natl Acad. Sci. USA* **95**, 3902–3907 (1998).
- Jones, C. *et al.* Expression profiling of purified normal human luminal and myoepithelial breast cells: identification of novel prognostic markers for breast cancer. *Cancer Res.* **64**, 3037–3045 (2004).
- Carter, W. G., Kaur, P., Gil, S. G., Gahr, P. J. & Wayner, E. A. Distinct functions for integrins alpha 3 beta 1 in focal adhesions and alpha 6 beta 4/bullous pemphigoid antigen in a new stable anchoring contact (SAC) of keratinocytes: relation to hemidesmosomes. *J. Cell Biol.* **111**, 3141–3154 (1990).
- Shackleton, M. *et al.* Generation of a functional mammary gland from a single stem cell. *Nature* **439**, 84–88 (2006).
- Li, Y. *et al.* Evidence that transgenes encoding components of the Wnt signaling pathway preferentially induce mammary cancers from progenitor cells. *Proc. Natl Acad. Sci. USA* **100**, 15853–15858 (2003).
- Goodell, M. A., Brose, K., Paradis, G., Conner, A. S. & Mulligan, R. C. Isolation and functional properties of murine hematopoietic stem cells that are replicating *in vivo*. *J. Exp. Med.* **183**, 1797–1806 (1996).
- Zhou, S. *et al.* The ABC transporter Bcrp1/ABCG2 is expressed in a wide variety of stem cells and is a molecular determinant of the side-population phenotype. *Nature Med.* **7**, 1028–1034 (2001).
- Spangrude, G. J. & Johnson, G. R. Resting and activated subsets of mouse multipotent hematopoietic stem cells. *Proc. Natl Acad. Sci. USA* **87**, 7433–7437 (1990).
- Uchida, N. *et al.* ABC transporter activities of murine hematopoietic stem cells vary according to their developmental and activation status. *Blood* **103**, 4487–4495 (2004).
- Bhattacharya, S. *et al.* Direct identification and enrichment of retinal stem cells/progenitors by Hoechst dye efflux assay. *Invest. Ophthalmol. Vis. Sci.* **44**, 2764–2773 (2003).
- Hierlihy, A. M., Seale, P., Lobe, C. G., Rudnicki, M. A. & Megoney, L. A. The post-natal heart contains a myocardial stem cell population. *FEBS Lett.* **530**, 239–243 (2002).
- Alvi, A. J. *et al.* Functional and molecular characterisation of mammary side population cells. *Breast Cancer Res.* **5**, R1–R8 (2003).
- Smith, G. H. Label-retaining epithelial cells in mouse mammary gland divide asymmetrically and retain their template DNA strands. *Development* **132**, 681–687 (2005).
- Glimm, H., Oh, I. & Eaves, C. Human hematopoietic stem cells stimulated to proliferate *in vitro* lose engraftment potential during their S/G₂/M transit and do not reenter G₀. *Blood* **96**, 4185–4193 (2000).
- Stingl, J., Emerman, J. T. & Eaves, C. J. in *Methods in Molecular Biology: Basic Cell Culture Protocols* (eds Helgason, C. D. & Miller, C. L.) 249–263 (Humana, New Jersey, 2005).
- Young, L. J. T. in *Methods in Mammary Gland Biology and Breast Cancer Research* (eds Ip, M. M. & Asch, B. B.) 67–74 (Kluwer/Plenum, New York, 2000).
- Szilvassy, S. J., Nicolini, F. E., Eaves, C. J. & Miller, C. L. in *Methods in Molecular Medicine: Hematopoietic Stem Cell Protocols* (eds Jordon, C. T. & Klug, C. A.) 167–187 (Humana, New Jersey, 2002).

Supplementary Information is linked to the online version of the paper at www.nature.com/nature. A summary figure is also included.

Acknowledgements This work was supported by grants from the Canadian Stem Cell Network and Genome BC/Canada. J.S. held Postdoctoral Fellowships from the Canadian Breast Cancer Foundation (BC/Yukon Chapter) and the Natural Sciences and Engineering Research Council of Canada; P.E. held a Stem Cell Network Studentship; I.R. and D.C. held British Columbia Cancer Foundation Summer Studentships; and M.S. held a Scholarship from the National Health and Medical Research Council of Australia. The authors thank the Ontario Genomics Innovation Centre for performing the microarrays, the Terry Fox Laboratory FACS Facility for assistance in cell sorting, G. Edin and K. M. Saw for technical assistance, and A. Eaves, S. Aparicio, C. Fisher and D. Kent for scientific discussion.

Author Contributions J.S., P.E., I.R. and D.C. performed most of the experiments described in the manuscript. M.S. and F.V. performed some of the single cell transplants. H.I.L. analysed the microarray data and J.S., P.E. and C.J.E. designed the studies and wrote the manuscript.

Author Information The microarray data can be accessed online at StemBase (<http://www.scgp.ca:8080/StemBase/>) and at the Gene Expression Omnibus (series accession number GSE3711) at <http://www.ncbi.nlm.nih.gov/geo/query/acc.cgi?acc=GSE3711>. Reprints and permissions information is available at ngp.nature.com/reprintsandpermissions. The authors declare no competing financial interests. Correspondence and request for materials should be directed to C.J.E. (ceaves@bccrc.ca).